SPARC-BD-07/004
10 October 2007

Generation of Ultra-Short, High Brightness Electron Beams for Single Spike SASE FEL Operation

J. B. Rosenzweig, G. Andonian, M. Dunning, A. Fukusawa, E. Hemsing, P. Musumeci, B.O'Shea, C. Pellegrini, S. Reiche
UCLA Department of Physics and Astronomy
L. Faillace, A. Marinelli, L. Palumbo
Università di Roma "La Sapienza" and INFN-LNF, Frascati
D. Alesini, M. Ferrario, M. Boscolo, B. Spataro, C. Vaccarezza
INFN-LNF, Frascati
V. Petrillo
Universita' di Milano and INFN-MI, Milano
L. Giannessi, C. Ronsivalle
ENEA, Frascati

Abstract

It has been suggested recently, that one should investigate the possibility of using an ultra-short beam, as short as one cooperation length and with very small charge, to drive short wavelength (*i.e*. X-ray) FELs. Such beams have very high brightness, and thus drive short gain length FELs. With short gain lengths come ever shorter cooperation lengths. In order to arrive at single spike operation— i.e. with the beam length roughly equal to a cooperation length — in such an X-ray FEL, the beam must therefore be extremely short. We have therefore investigated the creation, through initial velocity bunching at low energy and subsequent chicane bunching, of ultra-low-charge (≤ 1 pC) beams of sufficient quality to support strong FEL gain in two examples, the SPARX FEL and the LCLS. In both cases we find that we find that these beams can drive the FEL in single spike mode; one may therefore obtain SASE sources of coherent X-rays that are both quite stable and have pulse lengths at or below 1 femtosecond. These modes are, further, accessible through changes only in running conditions, not in projected (i.e. not yet existing) hardware.

Generation of Ultra-Short, High Brightness Electron Beams for Single Spike SASE FEL Operation

J. B. Rosenzweig, G. Andonian, M. Dunning, A. Fukusawa, E. Hemsing, P. Musumeci, B.O'Shea, C. Pellegrini, S. Reiche
UCLA Department of Physics and Astronomy
L. Faillace, A. Marinelli, L. Palumbo
Università di Roma "La Sapienza" and INFN-LNF, Frascati
D. Alesini, M. Ferrario, M. Boscolo, B. Spataro, C. Vaccarezza
INFN-LNF, Frascati
V. Petrillo
Universita' di Milano and INFN-MI, Milano
L. Giannessi, C. Ronsivalle
ENEA, Frascati

Introduction

It has been suggested recently in [1,2] that one should investigate the possibility of using an ultra-short beam, as short as one cooperation length and with very small charge, to drive short wavelength (*i.e.* X-ray) FELs [3,4]. Such beams have very high brightness, and thus drive short gain length FELs [5]. With short gain lengths come ever shorter cooperation lengths. In order to arrive at single spike operation [6] — i.e. with the beam length roughly equal to a cooperation length — in such an X-ray FEL, the beam must therefore be extremely short. We have therefore investigated the creation, through initial velocity bunching [7,8] at low energy and subsequent chicane bunching [9], of ultra-low-charge (≤ 1 pC) beams of sufficient quality to support strong FEL gain in two examples, the SPARX FEL [10] and the LCLS [2]. In both cases we find that we find that these beams can drive the FEL in single spike mode; one may therefore obtain SASE sources of coherent X-rays that are both quite stable and have pulse lengths at or below 1 femtosecond. These modes are, further, accessible through changes only in running conditions, not in projected (i.e. not yet existing) hardware.

This note is organized as follows: we first quantitatively review the beam requirements that such a novel operating regime imply. We then work backwards through the machine to give insight into the constraints of ultra-short pulse operation. This inquiry proceeds first through the chicane compressor. We discuss the requirements on the beam before chicane compression given a certain final expected bunch length and energy spread. We then go through the exercise of generating such beams, through a combination of launching ultra-short, very low charge beams in the photoinjector, employing scaling laws to quickly determine the operating point of the device, and its expected performance. We then use a velocity bunching scheme to arrive at the needed beam parameters. The process of electron beam creation and velocity bunching is simulated with PARMELA, while the final compression is modeled using ELEGANT. Finally, we verify the performance of the FEL systems using GENESIS.

From the viewpoint of the beam, we find a wide variety of advantages in operation with ultra-low charge. First, of course, is that ultra-short beams are possible, along with low emittances — in other words, high brightness electron beams naturally result from the photoinjector [11]. In addition, there are a number of problems which are almost entirely mitigated in this scenario, having to do with the beam's interaction with its environment. These issues, which include coherent synchrotron radiation (CSR) [12,13] in the chicane compressor as well as surface roughness and resistive wall wakes in the undulator vacuum wall [14,15,16], will be discussed in a subsequent work. This follow-on work will also discuss the challenges and opportunities for experimentally realizing operation of the beam in this environment.

FEL requirements

At short wavelengths, we may assume that the FEL performance is approximately described by 1D theory [17]. In this case, we begin with the 1D dimensionless gain parameter, which is given by

$$\rho_{1D} = \left[\frac{JJ(K_{rms})K_{rms}k_p}{4k_u}\right]^{2/3}, \tag{1}$$

where: $k_u = 2\pi/\lambda_u$ is the undulator wavenumber; $K_{rms} = e\sqrt{\langle B_u^2\rangle}\big/k_u m_e c$ is the rms undulator parameter; $JJ(K_{rms})$ is the coupling factor, which is slightly below unity in our planar undulator cases; and $k_p = \sqrt{4\pi r_e n_b/\gamma^3} = \sigma_x^{-1}\sqrt{2I_b/I_0\gamma^3}$ ($I_0 = ec/r_e \approx 17$ kA) is the relativistic beam plasma frequency.

The one-dimensional exponential gain length is given by

$$L_{g,1D} = \frac{\lambda_u}{4\pi\sqrt{3}\rho_{1D}}, \tag{2}$$

and the cooperation length, defined as the slippage distance over one gain length is

$$L_{c,1D} = \frac{\lambda_r}{4\pi\sqrt{3}\rho_{1D}}, \tag{3}$$

as the radiation overtakes the beam electrons by one radiation wavelength,

$$\lambda_r \cong \frac{\lambda_u}{2\gamma^2}\left[1+K_{rms}^2\right], \tag{4}$$

per undulator period. For single spike operation, the bunch length should obey

$$\sigma_{b,SS} < 2\pi L_{c,1D} = \frac{\lambda_r}{2\sqrt{3}\rho_{1D}} \tag{5}$$

In the case of SPARX design parameters [9], for operation at $\lambda_r = 3$ nm, $\rho_{1D} = 1.8\times10^{-3}$, and a single spike bunch length is estimated as $\sigma_{b,SS} = 0.48$ µm (1.6 fsec).

Note that the ρ-parameter is weakly dependent on the quantity that we intend to change in this study, the beam density n_b, as $\rho_{1D} \propto (n_b)^{1/3} \propto (I_b/\varepsilon_n)^{1/3}$. In any case we shall see that for very low charges, it is possible to obtain operating conditions in which the current decreases in comparison to standard operation, while the normalized emittance ε_n decreases further. Thus the ρ-parameter increases and the gain length decreases and one may operate a given saturating (in standard design case) FEL deeper in saturation.

Compression scaling

The compression processes that we employ in creating the final beams are of two types, velocity bunching at low (~5 MeV) energy and chicane bunching (usually two stages) at high (>500 MeV) energy. Because longitudinal space charge dominates the beam dynamics in velocity bunching (just as the transverse space-charge dominates the beam size in emittance compensation dynamics, see next section), one may deduce the scaling for the bunch length after velocity bunching, in a given design scenario, to be $\sigma_\varsigma \propto Q^{1/3}$. On the other hand, for chicane bunching at high energy, in the limit of low charge that we are examining, collective effects are strongly diminished compared to standard cases. In this case, the derivation of scaling laws concerning compression is also straightforward.

If we consider for the moment the limit of vanishing "slice" energy spread, the initial momentum distribution as a single-valued function of longitudinal coordinate ζ before the first chicane compressor is approximately [18]

$$p_z(\zeta) \cong p_{\max}\sin(k_{RF}\zeta) \cong p_0\left[1-\cot(\phi_0)k_{RF}\delta\zeta-\tfrac{1}{2}\left(k_{RF}\delta\zeta\right)^2\right]. \tag{6}$$

Here, $k_{RF}=2\pi/\lambda_{RF}$ is the RF wavenumber, ϕ_0 is the reference particle's RF phase, $\delta\zeta=\zeta-\phi_0/k_{RF}$, and we have taken for a linac accelerating section of length L_{acc} the maximum achievable momentum to be approximately $p_{\max}c \cong qE_0L_{acc}$. The first momentum deviation term on the right hand side of Eq. 6 is the linear chirp, which can be partly or completely removed by the action of the chicane.

We must also add a "thermal" or uncorrelated momentum spread $\sigma_{\delta p,th}=\sqrt{\delta p_{th}^2}/p_0$, which can be deduced from simulations, to the correlated momentum given in Eq. 6. This term dominates the final bunch length for ultra-short beams. To describe the situation before the chicane, it is useful to employ the second moments of the distribution:

$$\left\langle \delta\zeta^2 \right\rangle = \sigma_\zeta^2, \tag{7}$$

$$\frac{\left\langle \delta p^2 \right\rangle}{p_0^2} = \frac{\left(k_{RF}\sigma_\zeta\right)^4}{2} + \cot^2(\phi_0)\left(k_{RF}\sigma_\zeta\right)^2 + \sigma_{\delta p,th}^2, \quad \text{and} \tag{8}$$

$$\frac{\left\langle \delta\zeta \cdot \delta p \right\rangle}{p_0} = -\sigma_\zeta \cot(\phi_0)\left(k_z\sigma_\zeta\right). \tag{9}$$

The chicane is employed to partially or fully remove the correlation between the deviation in longitudinal position and momentum error $\delta p = p - p_0$.

Usually, one is restricted to considering partial compression, so that a linear chirp remains, which can be taken out using post-acceleration, with phase chosen back of crest. In the case of an ultra-short initial beam, where $\sigma_\phi = k_{RF}\sigma_\zeta << 1$, one may completely compress, to obtain the shortest possible beam and highest current. This compression may be performed at the final FEL energy, or as is more typical, at a lower energy, in which case the post-acceleration diminishes the relative momentum spread by the ratio of the chicane-to-final momenta.

With the assumption of full (and significant, meaning $\delta p_{th}/p_0 << k_{RF}\sigma_\xi \cot\phi_0$) compression, the chicane must have a longitudinal dispersion of [17]

$$R_{56} = \frac{k_{RF}\sigma_\xi^2 \cot(\phi_0)}{\frac{1}{2}\left(k_{RF}\sigma_\xi\right)^4 + \left(k_{RF}\sigma_\xi\right)^2 \cot^2(\phi_0) + \sigma_{\delta p,th}^2} \underset{\substack{k_{RF}\sigma_\xi << 1 \\ \delta p_{th}/p_0 << k_{RF}\sigma_\xi \cot\phi_0}}{\Rightarrow} \frac{1}{k_{RF}\cot(\phi_0)} = \frac{\lambda_{RF}\tan(\phi_0)}{2\pi}. \quad (10)$$

Under this condition the compression (final-to-initial bunch length) ratio is given by

$$\frac{\sigma_\xi^*}{\sigma_\xi} = \sqrt{\frac{\frac{1}{2}\left(k_{RF}\sigma_\xi\right)^4 + \sigma_{\delta p,th}^2}{\frac{1}{2}\left(k_{RF}\sigma_\xi\right)^4 + \sigma_{\delta p,th}^2 + \left(k_{RF}\sigma_\xi\right)^2 \cot^2(\phi_0)}} \cong \frac{\sigma_{\delta p,th}}{\sqrt{\sigma_{\delta p,th}^2 + \left(k_{RF}\sigma_\xi\right)^2 \cot(\phi_0)}}. \quad (11)$$

Note that in the limit of an initially long beam, one has the scaling $\sigma_\xi^* \propto k_{RF}\sigma_\xi^2$; an already short beam can be made much shorter. In the limit we consider here, however, the bunch length is limited by the relative thermal momentum spread $\sigma_{\delta p,th}$. This quantity is set by the process of velocity bunching, in which space-charge gives thermal-like distortions to the phase space. In the case of the simulations we have performed, discussed below, the rms uncorrelated energy spread after velocity bunching is $\sim 35\left[Q(\text{pC})\right]^{1/3}$ keV, a value which is then invariant during subsequent acceleration. We note in this regard that compression at the highest energy thus produces the shortest beams.

At this point, a numerical example, that of the SPARX FEL operated at 2 GeV, serves to illustrate the demands that single-spike operation make on the bunch length upstream of the chicane. For the single-spike bunch length as calculated above, we should have an rms bunch length at the FEL of $\sigma_\xi^* \cong 480$ nm. Such a bunch length would be possible according to Eq. 11, compressing at full energy, and choosing ϕ_0=67° in S-band RF (2856 MHz), with a pre-chicane bunch length of σ_ξ =9 μm, implying a factor of 20 in compression. With these conditions, we must examine the rms momentum spread in the beam, to ensure consistency with the condition

$$\sigma_{\delta p} \cong \cot(\phi_0)\left(k_z\sigma_\xi\right) << \rho_{1D}. \quad (12)$$

With S-band RF, we have $\sigma_{\delta p} \cong 2.1\times10^{-4}$ and $\rho_{1D} > 1.8\times10^{-3}$ (this is the nominal SPARX design value, which may be enhanced in higher brightness operation) so Eq. 12 is satisfied.

We shall see below that the energy spread is not significantly enhanced during the chicane bunching due CSR. In order to explain this, we can use the simple model recently given by Bosch [19] for estimating the maximum energy loss per electron, which occurs near the beam longitudinal center. For a maximum current of $I_{\max}$, the rms energy loss is approximately

$$\sigma_E = \frac{Z_0 I_{\max}}{4\pi}\ln\left[\frac{\sigma_z\gamma^3}{R\sqrt{2\pi}}\right]. \quad (13)$$

Here $Z_0 = 377\ \Omega$ is the impedance of free space, and R is the bend radius of curvature in the chicane magnets. In order to achieve the compression, the correct $R_{56} \cong \frac{4}{3} R\theta_b^3$ [17] factor mush be chosen. Taking, consistent with previous SPARX designs, a magnet bend angle of $\theta_b = 25$ mrad (1.43°), we have R=830 m in the SPARX case. With these design parameters, we obtain $\sigma_{\delta p} \cong \sigma_E / E \cong 10^{-5}$. This is much smaller than the pre-existing momentum spread, and therefore is not inherently dangerous. One must, however, check that the radiative energy loss due to CSR inside of the chicane does not cause significant emittance growth. We discuss this issue in the next section.

In the case of velocity bunching at low energy, the minimum compression ratio is not subject to the considerations above, as it is limited by space-charge effects. Through simulations, we have found that this ratio is, for short, longitudinal space-charge dominated beams (i.e. not subject to RF curvature limits), approximately constant at 0.1. This constant ratio is expected, as the launch value of the (laser) rms length must also scale as $\sigma_0 \propto Q^{1/3}$. Thus the beam launched from the gun should have a pulse length of $\sigma_0 \cong 10\sigma_\zeta \cong 90$ μm (0.3 psec).

Photoinjector scaling

With the choice of bunch length dictated by the physics of the FEL and the two downstream compression processes, we can directly deduce the correct scaled beam charge Q that should be used to obtain the desired pulse length σ_0. We consider standard operation of the RF gun and emittance compensation solenoid, as is used in SPARC. In order to scale to shorter pulse length, the one must keep the beam density (and thus the beam plasma frequency $k_p \propto n_b^{1/2}$, which dictates the correct emittance compensation dynamics) constant [8]. In the standard case (Ferrario operating point [20]), we have Q=1 nC and σ_0 =0.87 mm. In order to scale the beam density and aspect ratio correctly, we have the condition on the beam sizes, in all three dimensions, that $\sigma_i \propto Q^{1/3}$. Thus to obtain a bunch length one order of magnitude smaller, we should lower the charge by a factor of 1000, from 1 nC to 1 pC.

One can predict the behavior of the emittance in this case, as charge scaling in the Ferrario operating point has been studied extensively [21]. The contributions to the emittance scale as follows:

$$\text{Space charge, } \varepsilon_{x,sc} \propto k_p^2 \sigma_x^2 \propto Q^{2/3}, \tag{14}$$

$$\text{RF/chromatic aberration, } \varepsilon_{x,RF} \propto \sigma_z^2 \sigma_x^2 \propto Q^{4/3}, \tag{15}$$

$$\text{Thermal emittance, } \varepsilon_{x,th} \propto T_c^{1/2} \sigma_x \propto Q^{1/3}. \tag{16}$$

At very low charge, the "thermal" emittance due to the inherent spread in photoelectron transverse momentum indicated by a temperature T_c must dominate. To illustrate this point, we can write the emittance for this family of designs as follows

$$\varepsilon_n(\text{mm-mrad}) = \sqrt{a_1 Q(\text{nC})^{2/3} + a_2 Q(\text{nC})^{4/3} + a_3 Q(\text{nC})^{8/3}}, \tag{17}$$

where from simulation studies we have $a_1 = 0.111$, $a_2 = 0.18$, and $a_3 = 0.18$. With Q=1 pC, one has a thermally dominated emittance of 0.033 mm-mrad.

If there were no emittance growth in this scheme, one would have a final beam current of 250 A, and thus a brightness of $B = 2I/\varepsilon_n^2 = 4.5\times10^{17}$ A/m^2, which is *two orders of magnitude higher* than the value indicated for the nominal design. Indeed, we will find that there is a factor of two emittance growth due to space-charge during velocity bunching, but we will still obtain a beam with much higher brightness using this scheme.

One may estimate the emittance growth due to CSR energy loss using a simple calculation based on Bosch's heuristic model. Assuming the energy loss mainly arises (due to coherent edge radiation) at the magnet exit/entrance in bends 3/4, the minimized emittance growth due to uncancelled dispersion after the chicane may be estimated, in the SPARX case, as

$$\Delta\varepsilon_n \cong \gamma\sigma_{\delta p}^2 \frac{R\theta_b^3}{\sqrt{2}} \cong 6\times10^{-9} \text{ m-rad} \qquad (18)$$

Note that this is an order of magnitude smaller than the emittance one obtains after velocity bunching, thus explaining the lack of emittance growth observed in the simulations discussed in the next section.

Beam simulations

We consider two cases here, both with S-band injectors and linacs: SPARX, and the LCLS. The injector and velocity bunching sections are identical in both cases, and are simulated with UCLA PARMELA [22]. The downstream linac and compression simulations are performed with ELEGANT [23]. In the case of SPARX, the chicane compression is assumed to be performed at full energy, while in the LCLS case, the compression occurs at the planned second compressor.

Table 1. Summary of UCLA PARMELA simulations of ultra-low charge beam operation, with emittance compensation and velocity bunching.

Charge	1 pC (6.2E6 electrons)
Laser pulse length (full)	300 fsec
Gun maximum on-axis electric field	110 MV/m
Average traveling wave section field	13.5 MV/m
Initial laser beam radius (full)	100 microns
Thermal emittance	0.033 mm-mrad
Emittance after velocity bunching	0.062 mm-mrad
Final bunch length (rms)	9 μm (28 fsec)
Energy after velocity bunching section	17.9 MeV
Final relative momentum spread	0.31%

The injector parameters are summarized in Table 1. The beam dimensions are scaled simply from the standard Ferrario operating point by dividing by 10, yielding a charge diminished by a factor of 1000. The velocity bunching is effective at producing a bunch an order of magnitude shorter than the laser pulse. The performance of the combined emittance compensation/velocity bunching processes is described in Figs. 1-3, which display the evolution of the beam transverse envelope (controlled in part by solenoids wrapped around the linac section), bunch length, and emittance. It can be seen that velocity bunching is employed at the cost of some additional transverse (above thermal) emittance and longitudinal momentum spread, as discussed above. The parameters that resulted from this set of simulations are sufficient for the purpose of driving an FEL.

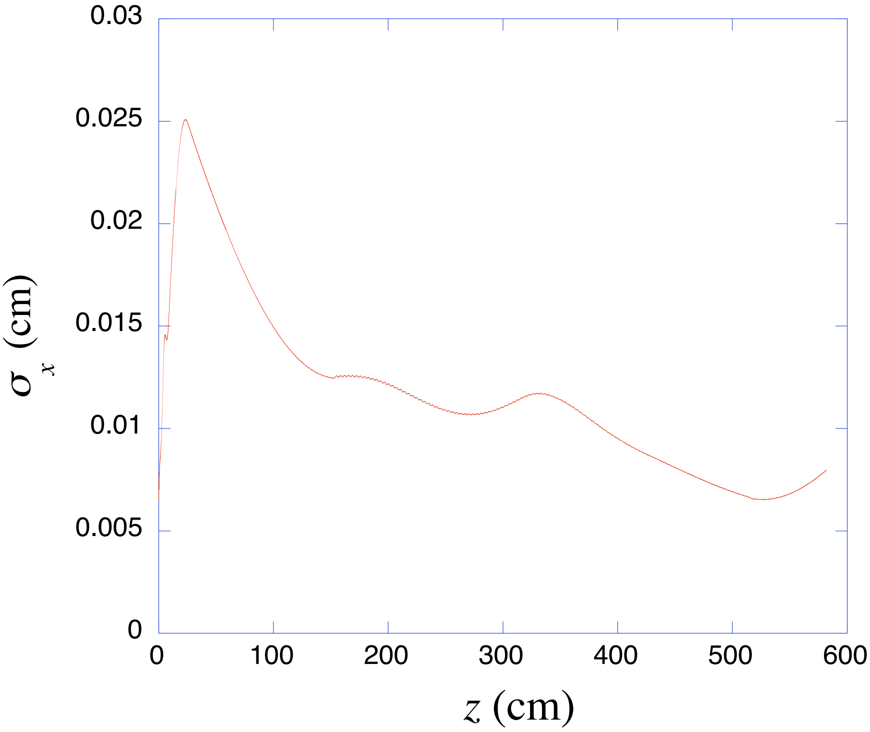

Figure 1. Evolution of beam transverse rms size during emittance compensation and velocity bunching.

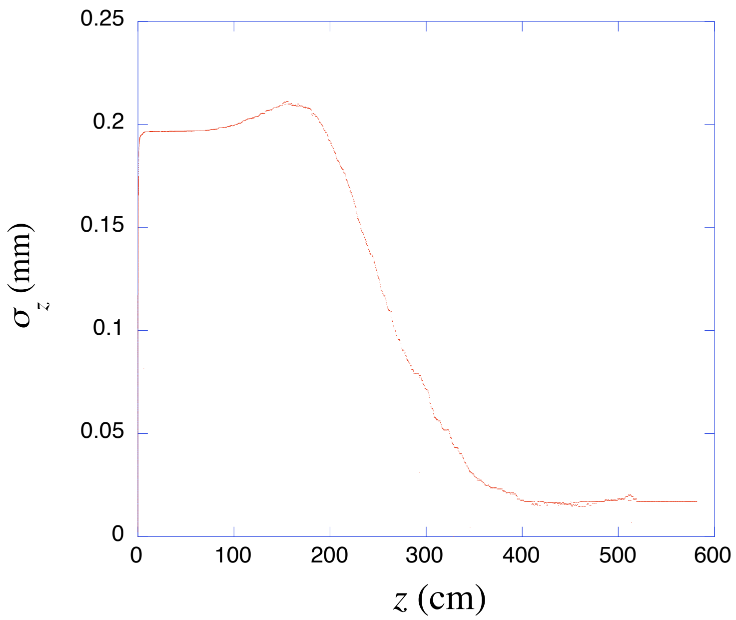

Figure 2. Evolution of beam longitudinal rms size during emittance compensation, velocity bunching.

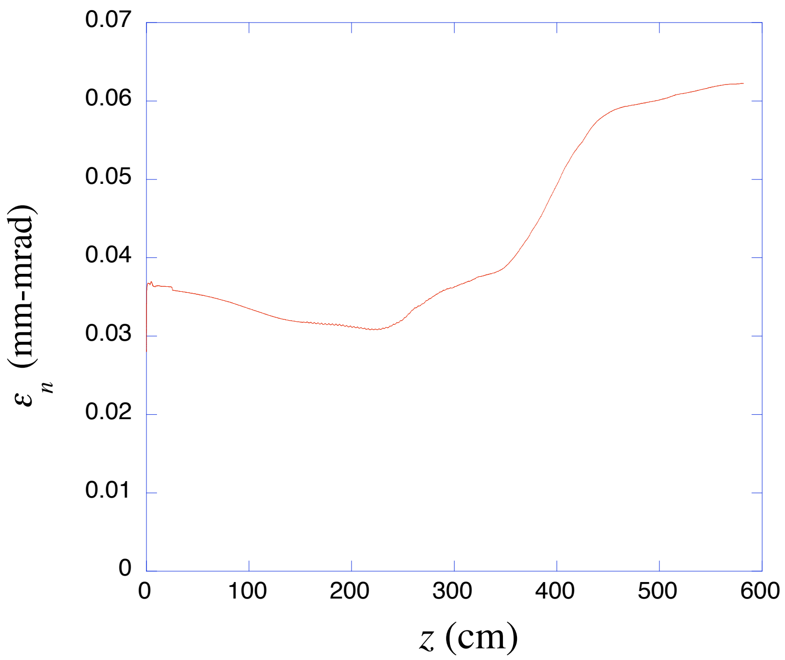

Figure 3. Evolution of beam rms emittance during emittance compensation and velocity bunching.

After the low energy section, we present two cases, one for SPARX, with a final energy of 2 GeV, and one for LCLS, at 14.5 GeV. The longitudinal phase spaces at final energies are displayed in Figs. 4. Note that we are compressing fully, which implies both maximum current and energy spread. The rms relative energy spread within the high current beam core in the two cases is given by $\sigma_{\delta p} = 2.4 \times 10^{-4}$ (SPARX) and $\sigma_{\delta p} = 1 \times 10^{-4}$ (LCLS), respectively. The beam current profiles in the two cases of interest are shown in Figs. 5. The rms bunch length for the SPARX example is given by $\sigma_z = 467$ nm (1.56 femtoseconds), while for the LCLS example $\sigma_z = 160$ nm (530 attoseconds). Thus we are able to approach the femtosecond frontier in electron beam creation using this method.

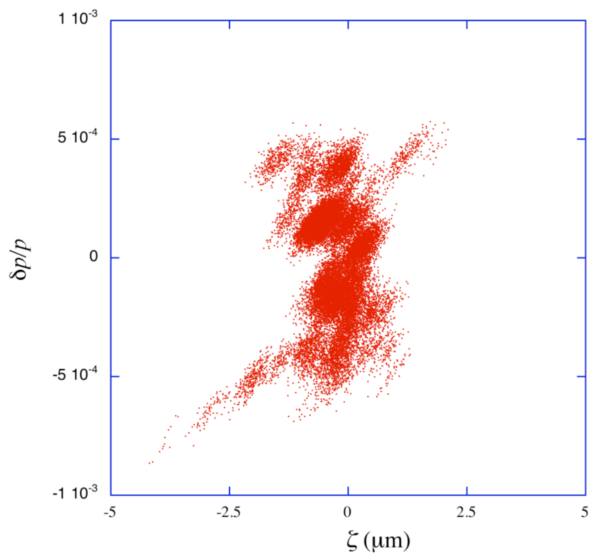

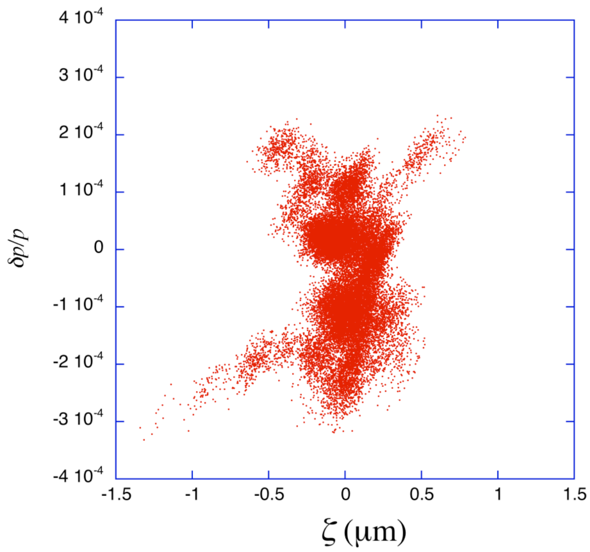

Figure 4. (left) Final longitudinal phase space at entrance of undulator, SPARX case; (right) final longitudinal phase space at entrance of undulator, LCLS case.

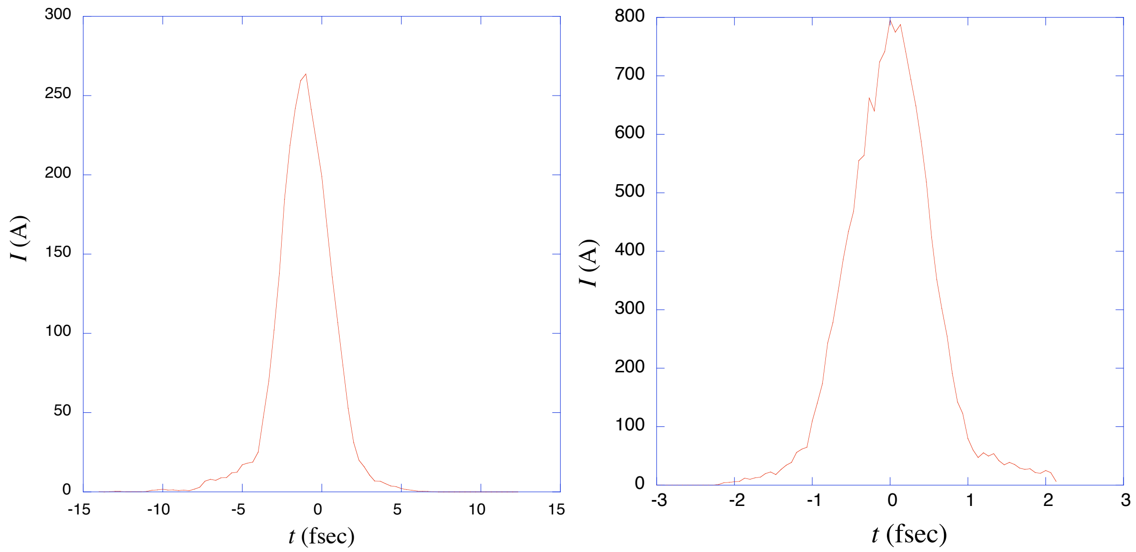

Figure 5. (left) beam current profile at entrance of undulator, SPARX case; (right) beam current profile at entrance of undulator, LCLS case.

A key advantage of ultra-low beam charge operation is that the beam emittance does not notably degrade due to collective effects during compression. Thus, with the values of the peak current obtained and a normalized emittance of $\varepsilon_n = 6.2\times10^{-8}$ m-rad, the beam brightness is greatly increased — it is $B = 1.35\times10^{17}$ A/m^2 in the SPARX case (slightly degraded from our estimate above due to emittance growth during velocity bunching). In the LCLS example, we have a final electron beam brightness of $B = 10^{18}$ A/m^2. In both cases, we have found over two orders of magnitude improvement in the brightness using ultra-low charge beams.

Free-electron laser simulations

We now complete the two experimental scenarios given above by simulating the performance of the respective FELs. The parameters of these simulations, performed with Genesis 1.3 [24], are given in Tables 2 and 3. We note that the undulator and electron beam focusing parameters are kept the same as in reference designs, despite the fact that they may no longer be optimum with such high brightness beams. In short, one might focus harder, as with smaller emittances, the maximum rms angles in the beam ($\sigma_\theta = \sqrt{\varepsilon_n/\beta}$) tolerated by the FEL are not reached without much stronger focusing (*i.e.* smaller β). On the other hand, the present exercise serves to show the ease in which the FEL designs may be adapted to employing ultra-low charge, ultra-high brightness beams. Other considerations also enter into the choice of focusing, such as diffraction, as discussed further below.

Table 2. Parameters for Genesis simulation of SPARX system with ultra-short beam.

Undulator wavelength λ_u	2.8 cm
Undulator strength K_{rms}	1.516
Resonant wavelength λ_r	3 nm
Focusing β-function	12.5 m
Dimensionless gain parameter ρ_{1D}	2.3×10^{-3}

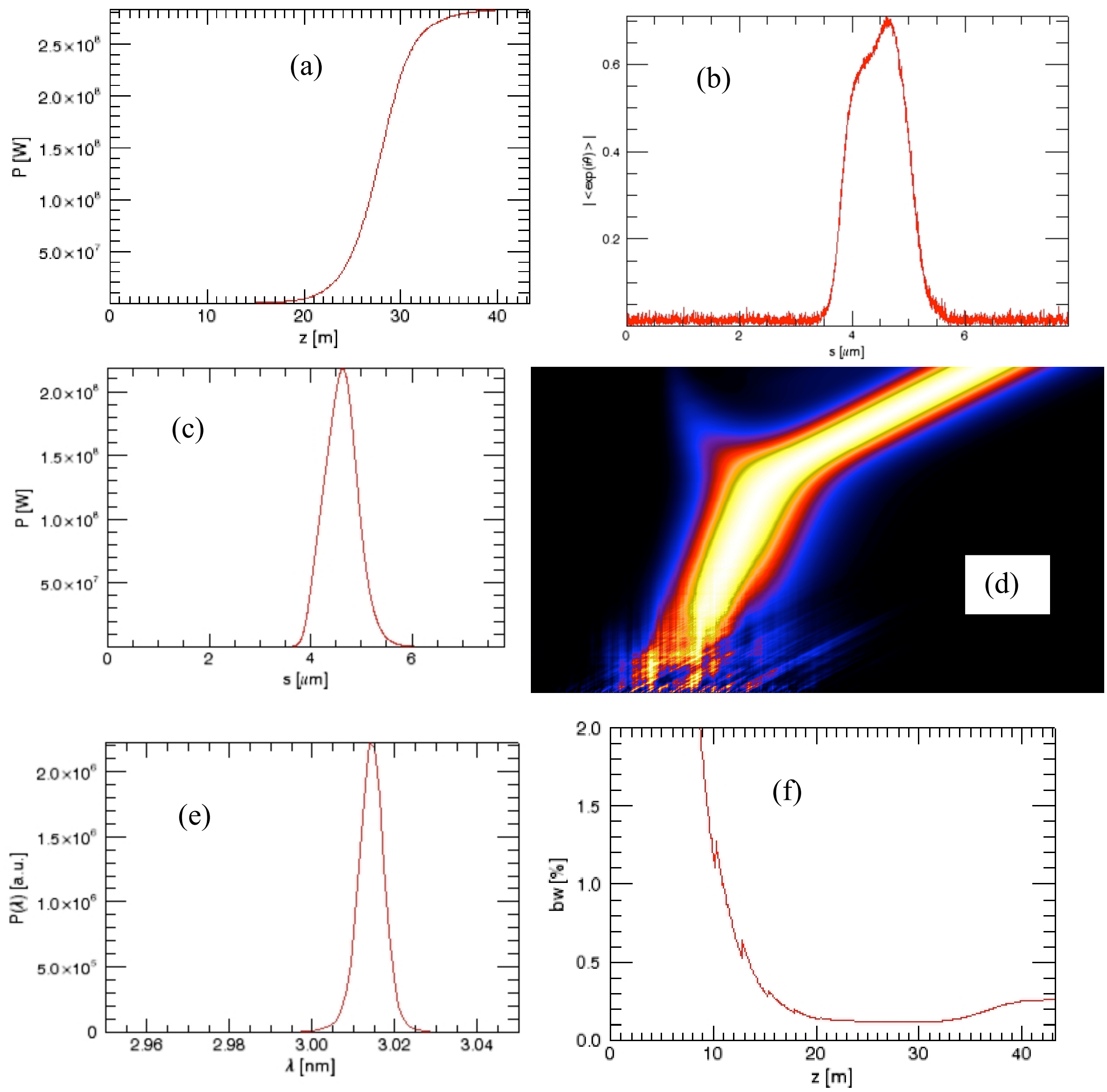

Figure 6. Results obtained from Genesis simulations, with input particles taken from the output of beam simulations, of the performance of the SPARX FEL. (a) Power vs. distance along the undulator z, (b) bunching factor at undulator exit, showing deep saturation, (c) peak power as a function of ζ at undulator exit, (d) power profile as a function of z (vertical) and ζ, (e) power spectrum at undulator exit, (f) relative bandwidth as a function of z.

Table 3. Parameters for Genesis simulation of LCLS system with ultra-short beam.

Undulator wavelength λ_u	3.0 cm
Undulator strength K_{rms}	2.2
Resonant wavelength λ_r	1.5 Å
Focusing β-function	25 m
Dimensionless gain parameter ρ_{1D}	2.0×10^{-3}

One may also see that the transverse beam size in the undulator, $\sigma_x = \sqrt{\beta\varepsilon_n/\gamma} = 14$ μm, is such that diffraction even plays a role in the gain process, as the "Rayleigh range" $Z_R = 4\pi\sigma_x^2/\lambda_r$ associated with the beam size (assuming the radiation mode size is the same) is only 83 cm! Because the assumed Z_R is less than the actual gain length, means that the radiation mode is larger than the electron beam. This further implies that, in the SPARX case, stronger focusing would not produce significantly enhanced performance.

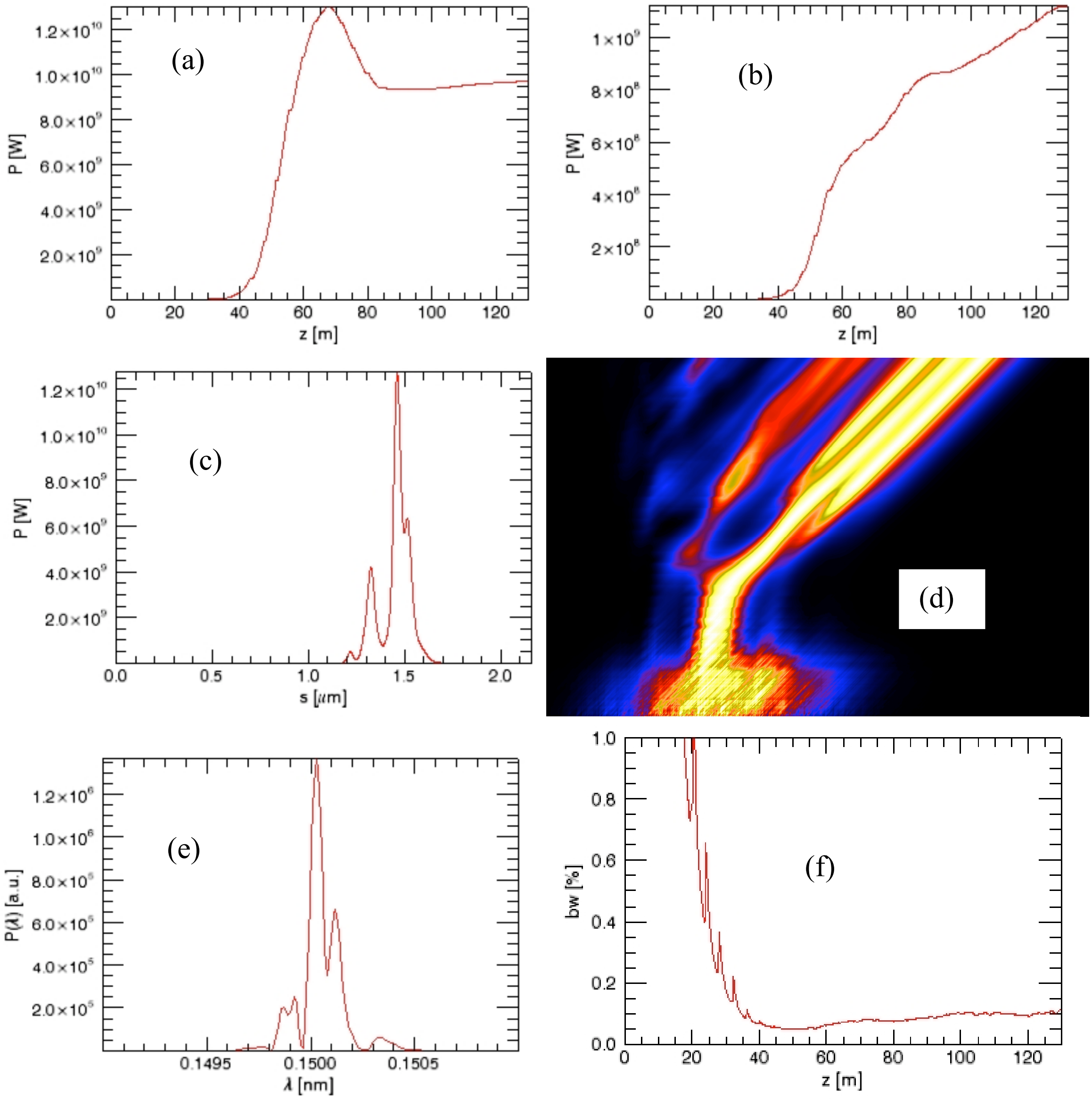

Figure 7. Results of Genesis simulations, using as input electrons taken form the output of beam simulations, concerning the performance of the LCLS FEL. (a) power vs. distance along the undulator z, (b) average power in simulation window vs. z, showing lack of saturation due to radiation after initial lasing, (c) power as a function of ζ at undulator exit, (d) power profile as a function of z (vertical) and ζ, illustrating growth of secondary spikes due to super-radiance (e) power spectrum at undulator exit (f) relative bandwidth vs. z.

In Figs. 7, we show a similar set of results for the LCLS case. In this scenario, the cooperation length is nearly an order of magnitude shorter, while the beam is compressed further by only a factor of 3. After saturation, the FEL pulse develops multiple spikes, which are due to super-radiant emission [25] from the bunched beam as it rotates in longitudinal phase space inside of the saturated FEL "bucket". This phase space rotation exists when the beam is so long that the radiation does not escape forward due to slippage. In this regard, we note that Fig. 7(c) bears a resemblance to Fig. 2 in Ref. 24. Still, as seen in Fig. 7(d), single spike behavior is observed during exponential gain. This is illustrated by the Figs. 8, where the temporal power profile and the wavelength spectrum just before saturation are given.

In order to avoid these problems, one may either shorten the active length of the undulator, or make the FEL gain slower. In the second case, in order to bring the system into single-spike operation, one needs only to "spoil" the emittance a bit (which is controlled easily by the laser spot size on the photocathode). In this regard, as an aside we note that the estimated emittance growth due to CSR in the LCLS case is actually smaller than in for SPARX case. In fact, one can see from Figs. 7 that the higher brightness beam produces a notably shortened gain length.

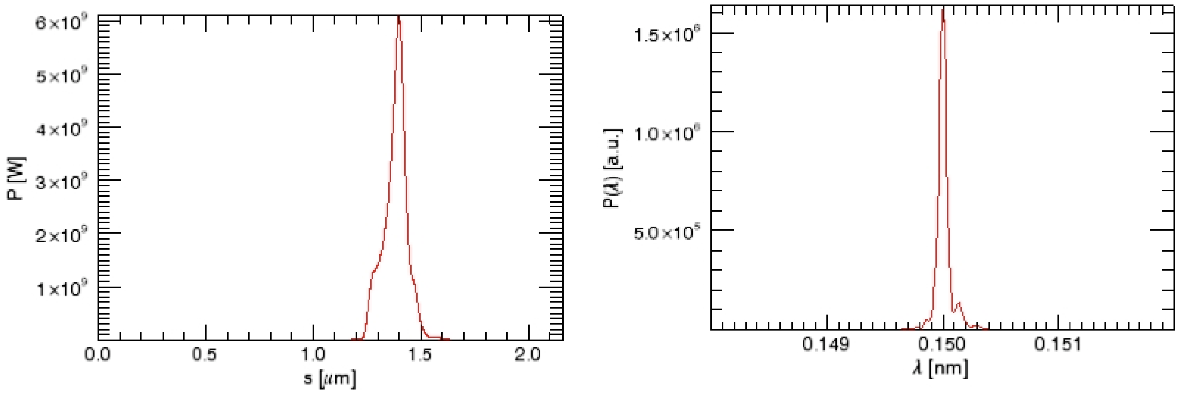

Figure 8. Results obtained from Genesis simulations of the LCLS FEL, as in Figs. 7, but quantities examined just previous to saturation: (left) power vs. ζ current profile as a function of ζ; (right) at undulator exit.

Conclusions and Future Work

As can be seen from the discussion given above, this scheme works very well, producing single spike operation in the SPARX FEL, and nearly single spike in the LCLS case. In order to degrade the emittance in the LCLS case, it would serve simply to make the beam spot larger on the cathode. It should be emphasized that in order to obtain the ultra-short, ultra-small Q beams using the nominal bunching mechanisms, one needs not use any additional hardware in both the SPARX and LCLS cases. In the end, single spike operation should give tremendous advantages not only in pushing the frontier of X-ray FEL pulses to time-resolution at the level of *atomic electron* motion, but in the statistical quality of these pulses.

In comparison to other schemes, such as the slit-spoiler method [26], chirped pulses [27], enhanced SASE [28], the ultra-low charge option has decided advantages. First, none of these competing schemes mitigates the collective effects in the linac and compression systems in the way foreseen for the ultra-low chare scheme. In addition, the other schemes do not produce a pedestal-free pulse. This may be a critical advantage in X-ray experimentation at free-electron laser facilities.

There are also clearly challenges in using these types of pulses in the context of existing or modified injectors and accelerators. First, we note that the total dark current obtained in high field operation of S-band photoinjectors tends to be on the 1 nC level. Thus integrating detectors such as screens (particularly just after the gun), will have some background issues. One may "clean up" the dark current using two anti-phased RF deflectors, separated by π (mod 2π) betatron phase advance, with collimators placed in between.

Just as interesting is the question of beam diagnostic resolution; one must be able to measure very small emittances and extremely short bunch lengths. We note in this regard that beam after velocity bunching will emit coherently (in, e.g., diffraction radiation) in the far IR. An even more compelling scenario is obtained for these beams after final compression, as they would emit (in, e.g., CER/CSR from the final chicane dipole) coherent visible to IR light. The expected signal, despite the low charge, is quite robust.

The issues associated with both dark current mitigation and beam observations and handling in the ultra-low charge, ultra-short case are discussed in a forthcoming note. This follow-on work also identifies possible measurements that one may make at the SPARC facility to investigate both the unique beam and FEL physics regimes that are accessed using the type of electron bunches discussed here.

References

[1] M. Ferrario et al., http://www.lnf.infn.it/acceleratori/sparc/technotes/bd/sparc_bd_07_003.pdf, May, 2007.
[2] C. Pellegrini, http://photonscience.slac.stanford.edu/pulse/uxss2007/talks/Pellegrini_SLAC-Pulse_june_07.pdf
[3] Linac Coherent Light Source Conceptual Design Report, SLAC-R-593, SLAC, 2002.
[4] TESLA Technical Design Report, TESLA FEL 2002-09, DESY, 2002.
[5] R. Bonifacio, C. Pellegrini, and L. Narducci, Opt. Commun. 50, 373 (1984).
[6] R. Bonifacio, L.D. Salvo, P.Pierini, N.Piovella, C. Pellegrini, Phys. Rev. Lett. 73, 70 (1994)
[7] L. Serafini and M. Ferrario, in *Physics of, and Science with, the X-Ray Free-Electron Laser,* edited by S. Chattopadhyay, M. Cornacchia, I. Lindau, and C. Pellegrini, AIP Conf. Proc. No. 581 (AIP, New York, 2001).
[8] S. G. Anderson, P. Musumeci, J. B. Rosenzweig, W. J. Brown, R. J. England, M. Ferrario, J. S. Jacob, M. C. Thompson, G. Travish, A. M. Tremaine, and R. Yoder , *Phys. Rev. ST-Accel. Beams* **8**, 014401 (2005).
[9] J.B. Rosenzweig, N. Barov and E. Colby, *IEEE Trans. Plasma Sci.* **24,** 409 (1996)
[10] C. Vaccarezza., et al., Proc. European Particle Accelerator Conf. 2006, 107 (JACOW, 2006).
[11] J.B. Rosenzweig and E. Colby, *Advanced Accelerator Concepts* p. 724 (AIP Conf. Proc. 335, 1995).
[12] S. Heifets, G. Stupakov, and S. Krinsky, *Phys. Rev. ST Accel. Beams* **5**, 064401 (2002).
[13] S. Reiche and J. B. Rosenzweig, *Phys. Rev. ST Accel. Beams* **6**, 040702 (2003).
[14] A. Mostacci, et al., "Review of Surface Roughness Effects on Beam Quality" in *The Physics and Applications of High Brightness Electron Beams,* Ed. J. Rosenzweig, L. Serafini and G. Travish (World Scientific, 2003)
[15] G. Stupakov, et al., *Phys. Rev. ST Accel. Beams* **2**, 060701 (1999).
[16] F. Zhou, et al., *Phys. Rev. Lett.* **89**, 174801 (2002)
[17] Zhirong Huang and Kwang-je Kim, *Phys. Rev. ST Accel. Beams* **10**, 034801 (2007)
[18] James Rosenzweig, in *Fundamentals of Beam Physics,* Oxford University Press, 2003.
[19] R. A. Bosch, *Phys. Rev. ST Accel. Beams* **10**, 050701 (2007).
[20] M. Ferrario, J.E. Clendenin, D.T. Palmer, J.Rosenzweig, and L. Serafini, in *The Physics of High Brightness Beams,* 534 (Eds. J. Rosenzweig and L. Serafini, World Scientific, 2000)
[21] M. Ferrario, W.D. Moeller, J.B. Rosenzweig, J. Sekutowicz and G. Travish, *Nucl. Instrum. Methods A*, **57** 98 (2006)
[22] E. Colby, UCLA PhD Thesis, FERMILAB-THESIS-1997-03 (FNAL, 1997)
[23] M. Borland, http://www.aps.anl.gov/asd/oag/oaghome.shtml.
[24] S. Reiche, Nucl. Instrum. Methods Phys. Res., Sect. A 429, 243 (1999).
[25] L. Giannessi, P. Musumeci, and S. Spampinati, *J. Appl. Physics* **98**, 043110 (2005).
[26] P. Emma et al., *Phys. Rev. Lett.* **92**, 074801 (2004).
[27] Z. Huang and S. Krinsky, *Nucl. Instrum. Methods A* **528**, 28 (2004)
[28] Alexander Zholents, *Phys. Rev. ST Accel. Beams* **8**, 040701 (2007).